

# Reconfigurable Shack–Hartmann sensor without moving elements

Raúl Martínez-Cuenca,<sup>1,2,\*</sup> Vicente Durán,<sup>1,2</sup> Vicent Climent,<sup>1,2</sup> Enrique Tajahuerce,<sup>1,2</sup> Salvador Bará,<sup>3</sup> Jorge Ares,<sup>4</sup> Justo Arines,<sup>4</sup> Manuel Martínez-Corral,<sup>5</sup> and Jesús Lancis<sup>1,2</sup>

<sup>1</sup>GROC-UJI, Departament de Física, Universitat Jaume I, 12071 Castelló, Spain

<sup>2</sup>Institut de Noves Tecnologies de la Imatge, Universitat Jaume I, 12071 Castelló, Spain

<sup>3</sup>Departamento de Física Aplicada, Universidade Santiago, 15782 Compostela, Galicia, Spain

<sup>4</sup>Departamento de Física Aplicada, Universidad de Zaragoza, 50009 Zaragoza, Spain

<sup>5</sup>Departament d'Òptica, Universitat de València, 46100 Burjassot, Spain

\*Corresponding author: rcuenca@fca.uji.es

Received January 28, 2010; revised March 15, 2010; accepted March 15, 2010;  
posted March 23, 2010 (Doc. ID 123489); published April 22, 2010

We demonstrate wavefront sensing with variable measurement sensitivity and dynamic range by means of a programmable microlens array implemented onto an off-the-shelf twisted nematic liquid crystal display operating as a phase-only spatial light modulator. Electronic control of the optical power of a liquid lens inserted at the aperture stop of a telecentric relay system allows sensing reconfigurability without moving components. Results of laboratory experiments show the ability of the setup to detect both smooth and highly aberrated wavefronts with adequate sensitivity. © 2010 Optical Society of America

OCIS codes: 110.1080, 280.4788, 070.6120.

Shack–Hartmann wavefront sensors (SHWSs) enable us to reconstruct the phase shape of an input light beam from the measurement of its wavefront local slopes [1]. A SHWS consists of a microlens array (MLA) that spatially samples the incoming wavefront, producing a focal spot pattern on an image sensor, typically a CCD. The wavefront gradient of the aberrated beam is then evaluated by measuring the displacements of the spot centroids with respect to their reference positions. The performance of a SHWS depends, among other parameters, on the number, size, distribution, and focal distance ( $f_m$ ) of the individual microlenses composing the MLA [2].

A desirable feature of a wavefront sensor is to allow for a tunable sensitivity (generally traded off against dynamic range), in order to optimize its performance according to the changing features of the wavefronts under test. Pyramid [3] as well as curvature sensors [4] are two well-known examples of devices in which this tuning can be accomplished with relative ease. SHWS can also be tuned by varying the focal length of the microlenses composing the MLA: in general, greater sensitivity can be obtained by increasing the microlens focal length (allowing the detection of smaller angular centroid displacements), while the dynamic range can be increased by reducing it (helping to avoid focal spot overlapping or prevent spot misidentification).

SHWSs with MLAs of tunable focal length have been reported, based on liquid-filled microlenses [5] or Fresnel microlenses codified onto a liquid crystal spatial light modulator (LC-SLM) [6,7]. In addition to a programmable focal length, adaptive SHWSs based on LC-SLMs are also able to change the geometry, size, and number of lenses of the MLA. Note, however, that a modification of the focal length generally requires an axial shift of the CCD to refocus the spot pattern, which otherwise may become unacceptably blurred. This movement, which in practice may in-

volve distances of the order of 100 mm, limits the acquisition speed of the detection system. Mechanical displacements can also alter the alignment of the apparatus, which, in terms of reliability, is critical for the determination of spot centroid displacements.

In this Letter we present a robust all-optical adaptive SHWS capable of handling wide changes of the MLA focal distance with no moving parts. It consists of a tunable focal length MLA codified as a set of diffractive microlenses on a phase-mostly twisted nematic LC-SLM, combined with a varifocal telecentric relay system (vTRES), which includes a liquid lens with electronic control over its optical power [8]. As the focal length of the MLA changes, the corresponding focal plane is imaged onto the CCD, which is kept at a fixed position by means of the vTRES. Thus, full electronic control of the design parameters is achieved without moving components. This allows adapting the SHWS to the characteristics of the incoming wavefront, a first step toward a really self-adjustable adaptive optical system operating in real time.

The SHWS is depicted in Fig. 1. Phase encoding of the MLA onto the LC-SLM provides a higher energetic efficiency than its amplitude counterpart. The

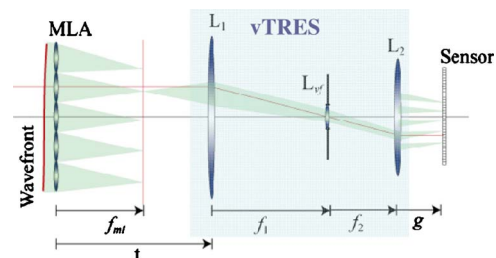


Fig. 1. (Color online) Reconfigurable SHWS. The optical power of the liquid lens and the lenslet focal length are matched so that the aerial spot pattern is imaged onto the sensor, which is kept at a fixed position, with constant magnification for all values of  $f_m$ .

twisted nematic liquid crystal display must be previously calibrated and inserted in a polarimetric arrangement to ensure phase-mostly operation [9]. Usually a maximum phase shift lower than  $2\pi$  can be achieved with commercial twisted nematic LC-SLM. Thus, a quantization algorithm must be applied to display the wrapped phases corresponding to the MLA. In its simplest configuration, the vTRES is composed of two lenses,  $L_1$  and  $L_2$ , in an afocal configuration, and a liquid lens,  $L_{vf}$ , with tunable optical power  $P_{vf}$ .  $L_{vf}$  is placed at the aperture stop of the relay, which is located at the common focus. The liquid lens we use is based on the electrowetting phenomenon with two isodensity liquids. A voltage signal leads to a change of the liquid-liquid interface, resulting in a change of the focal length [10]. The architecture of the relay is determined by the distance  $t$  between the MLA and  $L_1$ , the gap  $g$  between  $L_2$  and the CCD sensor, and the focal lengths of  $L_1$  and  $L_2$ ,  $f_1$  and  $f_2$ . The optical power of the liquid lens is adjusted for each value of the lenslet focal length to bring it into focus at the CCD, which is kept at a fixed position, the aerial spot distribution generated by the MLA. Mathematically, the required value for  $P_{vf}$  can be found by computing the  $ABCD$  matrix between the transverse planes containing the spot pattern and the CCD. We find

$$\begin{pmatrix} A & B \\ C & D \end{pmatrix} = \begin{pmatrix} -\frac{f_2}{f_1} & \frac{f_1^2(g-f_2) + f_1^2(P_{vf}f_1^2 - f_{ml} + t - f_1)}{f_1 f_2} \\ 0 & -\frac{f_1}{f_2} \end{pmatrix}. \quad (1)$$

The conjugation law, which reads as  $B=0$ , leads to the linear relation

$$P_{vf}(f_{ml}) = \frac{f_1 - t}{f_1^2} + \frac{f_2 - g}{f_2^2} + \frac{1}{f_1^2} f_{ml}. \quad (2)$$

Further, the geometrical magnification  $M$  is given by the coefficient  $A$ . In this way,  $M = -f_2/f_1$ . Since  $M \neq M(P_{vf})$ , the spot pattern is imaged with constant size at the CCD for every  $f_{ml}$ . The value for the magnification is chosen in such a way that the image of the spot pattern spreads over the whole active area of the CCD. In this way, the pattern is sampled with maximum resolution for all the possible configurations of the setup.

The performance of the SHWS is limited by the focusing capabilities of the twisted nematic LC-SLM and the liquid lens. At present, the optical power of a commercial liquid lens based on the electrowetting phenomenon can be electronically adjusted in a broad range covering  $-5$  to  $+15$  D. Note that, in accordance with Eq. (3), the range of focal lengths  $\Delta f_{ml}$  that can be brought into focus at the CCD by the liquid lens can be adjusted through the focal length  $f_1$ . Thus, it is the pixelated structure of the twisted nematic LC-

SLM that determines the ultimate SHWS specifications in terms of available measurement sensitivity and dynamic range.

In practical terms, once the sampling frequency over the aberrated waveform is decided, the pixel pitch determines the minimum achievable focal length. Specifically, the focal length of a diffractive lens consisting of several Fresnel zones is directly related to the outermost zone width  $\Delta r_N$  and the lenslet diameter through  $f_{ml} = d\Delta r_N/\lambda$ . For this case  $\Delta r_N$  is chosen as the pixel pitch. Higher-power diffractive microlenses cannot be properly codified because of the undersampling of outer zones. On the other hand, the long focal length regime is limited by imposing that the maximum phase excursion is reached only at the cell border and that no other point lies inside the lenslet aperture. Further, this value should be of the order of  $2\pi$  to ensure proper focusing capabilities of the codified lens. In this way, we estimate a maximum focal length of  $f_{ml} = d^2/8\lambda$ . Note that for a diffraction-limited situation, this restriction leads to a focal spot size that remains much smaller than the lenslet aperture in accordance with the Rayleigh resolution criterion.

Finally, it is also worth mentioning that we take advantage of the limited pupil diameter of commercial liquid lenses, usually a few millimeters, to block out light diffracted into the higher diffraction orders of the pixelated diffractive microlenses codified onto the twisted nematic LC-SLM. In terms of the speed of operation, the system supports continuous signal acquisition for video rates up to 30 frames/s.

The reconfigurable SHWS was experimentally tested in a wavefront measurement experiment with a MLA consisting of  $7 \times 7$  lenslets codified onto a twisted nematic LC-SLM (SONY LCX016ALC7) displaying  $832 \times 624$  pixels, pixel pitch  $32 \mu\text{m}$ . Each microlens was written over a  $19 \times 19$  pixel area. A four-level codification scheme for the wrapped phase corresponding to the MLA was applied as a maximum phase modulation slightly higher than  $3\pi/2$  was achieved for the wavelength of interest,  $\lambda = 530 \text{ nm}$ . A demagnifying vTRES ( $M \cong 0.8$ ) was built with geometrical parameters  $f_1 = t = 100 \text{ mm}$  and  $f_2 = g = 80 \text{ mm}$ . We used a liquid lens ARTIC 314, Vari-optics, with pupil diameter  $2.50 \text{ mm}$  and electronic control of the optical power in the range including  $\sim 2 \text{ D}$  and  $+10 \text{ D}$ . Finally, a 8-bit CCD camera, pixel size  $6.4 \mu\text{m}$ , was employed. In our implementation, we demonstrate a minimum and a maximum available lenslet focal length  $f_{ml} = 33 \text{ mm}$  and  $f_{ml} = 100 \text{ mm}$ , respectively, for the considered wavelength.

Figure 2 shows results of experiments. The SHWS was configured for maximum dynamic range to test wave aberrations in the optical beam generated through the collimation of the light emitted by a green LED with emission spectrum centered at  $530 \text{ nm}$ . Focused spots do not deviate significantly from the optical axis, and no information about aberrations in the collimation setup can be detected [Fig. 2(a)]. Wave aberrations become apparent when the SHWS is reconfigured into the maximum sensitivity

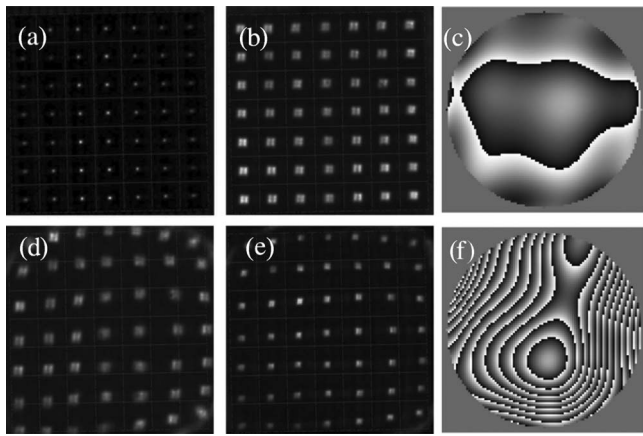


Fig. 2. Measurement of wave aberration for two modes of operation of the reconfigurable SHWS. See text for details.

mode [Fig. 2(b)]. From the spots we recover the wave aberration function in Fig. 2(c), which corresponds to a maximum phase delay (peak-to-valley) of  $1.7\lambda$ . Next, an aberrated plate and an ophthalmic lens were inserted into the light path. The plate was produced in photoresist, and it encoded aberrations with a shape and magnitude typical of human eyes [11]. The ophthalmic lens allows generating a higher amount of defocus. Spots are located outside of the field of view of the CCD sensor and almost overlap, causing centroid algorithms to fail [Fig. 2(d)]. The system was again reconfigured this time to operate with a lenslet focal length  $f_{ml}=60$  mm [Fig. 2(e)] allowing for a maximum measurement sensitivity compatible with keeping the focal spots within their corresponding windows. Visually it is obvious that the noise reduction in the SHWS spots in Fig. 2(e) permit a higher reliability in centroid location. The recovered  $12.2\lambda$  peak-to-valley wave aberration is shown in Fig. 2(f).

The calibration of this SHWS has the same general requirements as with a conventional one and can be done by following the usual procedures [2,11]. Some care must be taken when selecting the varifocal lens used in the vTRES in order to identify and account for possible power versus voltage hysteresis effects as

well as for any variable field distortion of the vTRES setup depending on the liquid lens power. None of these effects were relevant in our measurements.

In conclusion, the use of a varifocal telecentric relay system including a liquid lens with electronic control over its optical power provides a practical solution for operating a SHWS with tunable sensitivity and dynamic range with no moving parts. The possibility of imaging onto the CCD different axial planes around the nominal MLA focal plane is highly appealing even when working with fixed focal length microlens arrays, since highly aberrated wavefronts may induce enough defocus to axially displace their common focal plane, blurring the detected focal spots and thus reducing their signal-to-noise ratio. In both cases, reimaging the focal spots and achieving the proper sizing and irradiance allow a higher reliability in centroid location against noise.

This research was funded by the Spanish Ministerio de Ciencia e Innovación (MICINN), Spain, under the projects FIS2007-62217 and FIS2008-03884. We also acknowledge partial support from the Consolider Programme SAUUL CSD2007-00013 and project P1-1B2009-36 from the Convenio UJI-Bancaixa.

## References

1. R. V. Shack and B. C. Platt, *J. Opt. Soc. Am.* **61**, 656 (1971).
2. J. Ares, T. Mancebo, and S. Bará, *Appl. Opt.* **39**, 1511 (2000).
3. R. Ragazzoni, *J. Mod. Opt.* **43**, 289 (1996).
4. F. Roddier, *Appl. Opt.* **27**, 1223 (1988).
5. Y. Hongbin, Z. Guangya, C. F. Siang, L. Feiwen, and W. Shouhua, *J. Micromech. Microeng.* **18**, 105017 (2008).
6. L. Seifert, J. Liesener, and H. J. Tiziani, *Opt. Commun.* **216**, 313 (2003).
7. L. Zhao, N. Bai, X. Li, L. S. Ong, Z. P. Fang, and A. K. Asundi, *Appl. Opt.* **45**, 90 (2006).
8. R. Martínez-Cuenca, H. Navarro, G. Saavedra, B. Javidi, and M. Martínez-Corral, *Opt. Express* **15**, 16255 (2007).
9. V. Durán, J. Lancis, E. Tajahuerce, and M. Fernández-Alonso, *Opt. Express* **14**, 5607 (2006).
10. B. Berge and J. Peseux, *Eur. Phys. J. E* **3**, 159 (2000).
11. P. Rodríguez, R. Navarro, J. Arines, and S. Bará, *J. Refract. Surg.* **22**, 275 (2006).